

# Following beech litter decomposition with analytical pyrolysis: Inter-site variance and decomposition trends

---

## Abstract

Litter decomposition studies are key to understanding global carbon fluxes and soil formation. Analytical pyrolysis has the potential to provide insight into carbon transformations during decomposition. Most interestingly, this potential was not exploited yet. We report data of beech litter pyrolysis products of litter obtained from different sites in Austria and changes in pyrolysis products during litter decomposition

*Keywords:*

---

## 1. Introduction

Understanding plant litter decomposition processes is key to understanding the global carbon cycle, nutrient recycling and soil formation[1]. However, little is known about changes in the chemistry of high molecular weight substances during decomposition. The insufficient specificity of traditional methods to determine plant fibres[2] led to misinterpretation of decomposition dynamics. Analytical pyrolysis can provide a fast and cheap method to investigate chemical transformations of plant polymers during decomposition. However, while the use of analytical pyrolysis to quantify lignin and cellulose contents becomes more frequent, the full potential of a high definition interpretation of pyrograms is rarely used.

Analytical pyrolysis is frequently applied to characterize natural organic polymers in soil organic matter [and dissolved organic matter?]. Plant derived compounds make up an important part of pyrolysis products found. The relative abundances of such markers were shown to hold key information on past climates and decomposition conditions [3, 4, 5].

Only a handful of Pyr-GC/MS studies tracing changing pyrolysis markers during litter decomposition were published, none of them includes in depth. The only published work

directly studying the decay of plant leaf litter is [6]. [?] presents basic thermochemolysis data. Straw was incubated with n. Several studies monitor the decomposition of woody material with Pyr GC/MS [lit.] or litter/soils mixtures[lit.]. None of the studies mentioned above analysis decomposition trends of individual pyrolysis products.

While assignment to major compounds classes (like lignin or carbohydrate) based on pyrolysis reaction mechanisms is common, little is known on whether the composition of individual pyrolysis products within this groups yields information.

This study compares pyrograms of beech litter from different site after up to 15 month of climate chamber decomposition. Beech litter were reported for exceptionally slow decomposition rates (12% mass loss in the first year) in nature [?] and showed similar decomposition rates our climate chamber experiment. Therefore, we do not focus on the accumulation of recalcitrant compounds, but focus on how individual pyrolysis markers accumulate or deplete relative to their compounds of origin which might provide insight into changes in polymer condensation patterns.

## 2. Material and Methods

Beech litter from 4 different sites in Austria was collected in October 2008, cut to pieces <0.5 cm, homogenized, sterilized and inoculated with a common inoculate for all sites. Litter was incubated in a climate chamber at 15 °C and was kept at 60 % moisture [7]. Total mass loss after 15 month was between 7 and 12 %. Accumulated respiration after 6 month accounts for nn.to nn% of the litter carbon pool, after 15 month between n and n.

Pyrolysis-GC/MS was performed on a Pyroprobe 5250 pyrolysis system (CDS Analytical) coupled to a Thermo Trace gas chromatograph and a DSQ II MS detector (both Thermo Scientific) equipped with a carbowax column (Supelcowax 10, Sigma-Aldrich). 2-300 µg dried and finely ball-milled litter were heated to 600°C for 10 seconds in helium atmosphere. The temperature of the valve oven and the transfer line to the GC injection port were set to 250°C, a 10x split injection was applied with the injector heated to 240°C. Carrier gas flow was set to 1ml min<sup>-1</sup>. GC Oven temperature was constant at 50 °C for 2 minutes, followed

by an increase of 7°C/min to a final temperature of 260 °C, which was held for 15 minutes. The transfer line was heated to 270 °C. The MS detector was set for electron ionization at 70 EV, the ion source was heated to 270°C. Detection was set to cycle between m/z 20 and 300 with a cycle time of 0.3 seconds.

Peaks were assignment was based on NiSt 05 MS library and comparison with reference material measured. 128 peaks were selected for integration due to their hiht abundance or diagnostic value. For each peak between one and four mass fragments selected for high abundance and specificity were integrated (i.e. [4]). Peak areas are stated as % of the sum of all integrated peaks of a sample.

Pyrolysis products were assigned to their substances of origin by comparison to reference material, structural similarity and in accordance with literature ([8, 4, 9][more lit!]). We confirmed the identity of two products rarely reported for plant material (Phytol and 3-Hydroxypyridine) by the addition of reference material to the sample and comparison to MS libraries. Both substances were bought from Sigma-Aldrich (St. Louis, MO, USA).

$$\%lost = \frac{mean(actual\%)}{1 - \frac{carbonrespired}{initialcarboncontent}} - \%meaninitialcontent \quad (1)$$

## 2.1. Litter mass loss and respiration

## 2.2. Statistical analysis

All statistical analyses were performed with the software and statistical computing environment R using the R package “vegan” [10]. If not mentioned otherwise, results were considered significant, when p<0.05. All correlations refer to Pearson correlations. All data presented was tested for significant differences between harvests and litter types. Normal distribution assumed but could not be tested due to the small number of cases per treatment (n=4-5). A substantial part of variables had heterogeneous variances when tested with Levene’s test. Therefore, (one-way) Welch anova was used to calculate significant differences between harvests within each litter type and litter types within each harvest (alpha=0.05). For post-hoc group assignment, paired Welch’s t-tests with Bonferroni corrected p limits

were used. Principal component analysis was performed using vegan function “rda” scaling variables.

### 3. Results

#### 3.1. Mass loss and respiration

Accumulated mass loss during the first 181 days ranged between

#### 3.2. Pyrolysis products

A total of 128 peaks quantified including 28 phenolic, 11 nitrogen containing compounds and 42 carbohydrate derived compounds. Inter-site differences dominate both initial and incubated litter: In 127 peaks significant differences between litter from different sites was found during one time point, in 95 differences were significant in all 4 harvests. In 113 peaks significant differences between time points were found, but only 49 peaks had significant changes during incubation in more than two litter types.

#### 3.3. Lignin and other phenolic compounds

Of 38 phenolic pyrolysis products were identified, 15 of which had guaiacol-, 13 syringol-, and 10 non-methoxylated ring systems.

Guaiacol/Syringol (G/S) ratios were tightly (all  $R=0.68-0.94$ ,  $p<0.001$ ) correlated between the more abundant side chains (-H, -CH<sub>3</sub>, -CH<sub>2</sub>CH<sub>3</sub>, -CH=CH<sub>2</sub>, -CH<sub>3</sub>CH=CH<sub>2</sub>). This correlation is weaker or non-significant for less abundant side chains (-CHO, -CH<sub>2</sub>CH<sub>2</sub>CHO) due to higher variances in their detection.

Part of non-methoxylated phenols pyrolysis products (side chains -CH<sub>2</sub>CH<sub>3</sub>, -CH<sub>2</sub>CH<sub>2</sub>CH<sub>3</sub>, -CH<sub>3</sub>CH=CH<sub>2</sub>) show clear structural similarity to pyrolysis products of lignin, suggesting that they are pyrolysis products of p-hydroxypropanylphenol based lignin. Other side chains (-H, -CH<sub>3</sub>, -CHO) are less specific and are reported for other sources, although in small amounts. Furthermore, some of the phenolic compounds (i.e. hydroxyquinone) are not lignin derived.

In both syringol and guaiacol the ratio between the abundances of pyrolysis products is the same.

Guaiacol to Syringol ratios were constant over decomposition time. The ratios are different for G/S compounds with different side chains, probably due to changing MS responses of the compounds

Most important difference between sites were observed in the ratio between Guaiacol

The pattern of abundances of different side chains was the same for guaiacol and syringol derived compounds. Fig 4 shows that pairwise ratios between 5 different lignin side chains are highly significant in guaiacol and syringol lignin based pyrolysis products. However, there are some site-specific differences in these patterns: the abundance of -H and -CH<sub>3</sub> side chains relative to other side chains is different between the litter types, but consistent between guaiacol and syringol derivatives. Side chains with oxygen based functional groups were present, but in abundances much lower than the before mentioned.

[3, 4] use the Guaiacol+Syringol to C<sub>3</sub>-Guaiacol+Syringol ratio as an indicator for aerobic/anaerobic degradation.

### 3.4. N compounds

In total, 11 nitrogen containing compounds were identified, including two indole three pyridine and 5 pyrrole derivatives. 8 of them were strictly correlated to litter N content (all  $R > 0.8$ ,  $p < 0.001$ ). Two groups could be identified among them: indole and methylindole were highly correlated to each other ( $R = 0.98$ ,  $p < 0.05$  to  $0.001$ ), as were 6 pyridine and pyrrole derivatives (all  $R > 0.9$ ,  $p < 0.05$  to  $0.001$ ). Correlations between peaks of two groups were still high, but lower than within the groups ( $R = 0.77$ - $0.87$ ,  $p < 0.05$  to  $0.001$ ). Both groups show a continuous increase during litter decomposition: after 15 months pyridine and pyrrole derivatives increase by 8-20% of their initial content, indole and methylindole by 20-30% (fig. 8).

Two pyrolysis products show different trends: The abundance of 3-Hydroxypyrrole strongly (30-50%) decreases during first six months, then follows general N trend. N-methyl-pyrrole shows an increase between 5 and 35% (%TIC) during the first 6 months and remains stable thereafter (fig. 8).

### 3.5. Carbohydrates

In total, 42 carbohydrate derived pyrolysis products were identified either by their structure or by comparison to reference material. Unlike lignin or N compounds, carbohydrate pyrolysis products do not follow a common trend, but - reflecting the differences within this group. About a third of the peaks could not be identified but were assigned to carbohydrates because they are present reference pyrograms of carbohydrates, but not in other compounds.

Methylated cyclopentenone derivatives show an increase over decomposition, while derivative with keto- or hydroxy- side chains show decreases over decomposition.

Furanmethanol shows an especially high degradation rate, losing 15 to 30 % of its initial contribution to the total peak area over 15 months.

### 3.6. Other compounds

#### 3.6.1. Phytol

We found two compounds with terpenoid structure: Phytol is a chlorophyll derived C<sub>20</sub> alcohol mentioned as a pyrolysis product only by [? ]. We confirmed the compounds identity by comparison with commercially available material. Phytol is strongly depleted during decomposition in low-N sites (up to 50% of its relative peak area in OS and AK), but not in high-N sites (SW). (fig ??)

#### 3.6.2. Fatty acids

Three saturated fatty acids were found in litter pyrograms (14:0, 16:0, 18:0). The three fatty acids were also most abundant in THM analysis of this litter material (data not shown).

Initial content of fatty acids showed differences of up to 30 % between sites. For the three fatty acids found, between 15 and 50 % were degraded over 15 months, indicating that both accumulation and depletion occurs in certain sites.

#### 3.6.3. Long chained alkanes and alkenes

We found C<sub>25</sub>-C<sub>29</sub> alkanes and alkenes in our pyrograms. The two had different decomposition trends: While

## 4. Discussion

### 4.1. Inter-site variance during litter decomposition

We found that differences in litter pyrolysis products persist at least during early litter decomposition. Differences in Lignin side chains indicate different polymerization patterns in different sites.

### 4.2. Lignin side chains

Until now, studies following lignin degradation with Pyr-GC/MS were focusing on changes between the frequency of lignin pyrolysis products, only the ratio between guaiacol/syringol/phenol based ring system was investigated. We found substantial differences in the frequency of different lignin side chains between litter collected at different sites. We found that these differences remained nearly constant during during 15 month of litter decomposition.

### 4.3. Pyridine/Pyrrol to Indole ratio

The ration between indene and pyridine/pyrrol ring pyrolysis products drops during decomposition by about 20%. Initial differences between sites (OS is higher than the rest) remain. Increase in tryptophan content among amino acids in bacterial protein?

### 4.4. Lipophilic compounds

From our dataset, we see that (1) alkenes are accumulated

## 5. Conclusions

## 6. Acknowledgements

## References

- [1] C. E. Prescott, Litter decomposition: what controls it and how can we alter it to sequester more carbon in forest soils?, *Biogeochemistry* 101 (1-3) (2010) 133–149. doi:10.1007/s10533-010-9439-0.  
URL <http://www.springerlink.com/index/10.1007/s10533-010-9439-0>

- [2] R. D. Hatfield, S. F. Romualdo, Can Lignin Be Accurately Measured?, *Crop Science* 45 (3) (2005) 832–839.  
URL <http://crop.scijournals.org/cgi/doi/10.2135/cropsci2004.0238>
- [3] T. Kuder, M. A. Kruege, Preservation of biomolecules in sub-fossil plants from raised peat bogs – a potential paleoenvironmental proxy, *Organic Geochemistry* 29 (5-7) (1998) 1355–1368. doi:10.1016/S0146-6380(98)00092-8.  
URL [http://dx.doi.org/10.1016/S0146-6380\(98\)00092-8](http://dx.doi.org/10.1016/S0146-6380(98)00092-8)
- [4] J. Schellekens, P. Buurman, X. Pontevedra-Pombal, Selecting parameters for the environmental interpretation of peat molecular chemistry – A pyrolysis-GC/MS study, *Organic Geochemistry* 40 (6) (2009) 678–691. doi:10.1016/j.orggeochem.2009.03.006.  
URL <http://linkinghub.elsevier.com/retrieve/pii/S0146638009000680>
- [5] J. Schellekens, P. Buurman, I. Fraga, A. Martínez-Cortizas, Holocene vegetation and hydrologic changes inferred from molecular vegetation markers in peat, Penido Vello (Galicia, Spain), *Palaeogeography, Palaeoclimatology, Palaeoecology* 299 (1-2) (2011) 56–69. doi:10.1016/j.palaeo.2010.10.034.  
URL <http://linkinghub.elsevier.com/retrieve/pii/S0031018210006504>
- [6] J. Franchini, F. Gonzalez-Vila, J. Rodrigues, Decomposition of plant residues used in no-tillage systems as revealed by flash pyrolysis, *Journal of Analytical and Applied Pyrolysis* 62 (1) (2002) 35–43.  
URL [http://apps.isiknowledge.com/full\\_record.do?product=UA&colname=WOS&search\\_mode=C](http://apps.isiknowledge.com/full_record.do?product=UA&colname=WOS&search_mode=C)
- [7] W. Wanek, M. Mooshammer, A. Blöchl, A. Hanreich, A. Richter, Determination of gross rates of amino acid production and immobilization in decomposing leaf litter by a novel N-15 isotope pool dilution technique, *Soil Biology and Biochemistry* 42 (8) (2010) 1293–1302. doi:10.1016/j.soilbio.2010.04.001.  
URL <http://linkinghub.elsevier.com/retrieve/pii/S0038071710001331>
- [8] J. Ralph, R. D. Hatfield, Pyrolysis-GC-MS characterization of forage materials, *Journal*



of Agricultural and Food Chemistry 39 (8) (1991) 1426–1437. doi:10.1021/jf00008a014.

URL <http://pubs.acs.org/doi/abs/10.1021/jf00008a014>

[9] G. Chiavari, G. C. Galletti, Pyrolysis-gas chromatography/mass spectrometry of amino acids, Journal of Analytical and Applied Pyrolysis 24 (1992) 123– 137.

[10] J. Oksanen, F. G. Blanchet, R. Kindt, P. Legendre, R. O’Hara, G. L. Simpson, P. Slysos, M. H. H. Stevens, H. Wagner, vegan: Community Ecology Package. R packge version 1.17-9 (2011).

URL <http://cran.r-project.org/package=vegan>

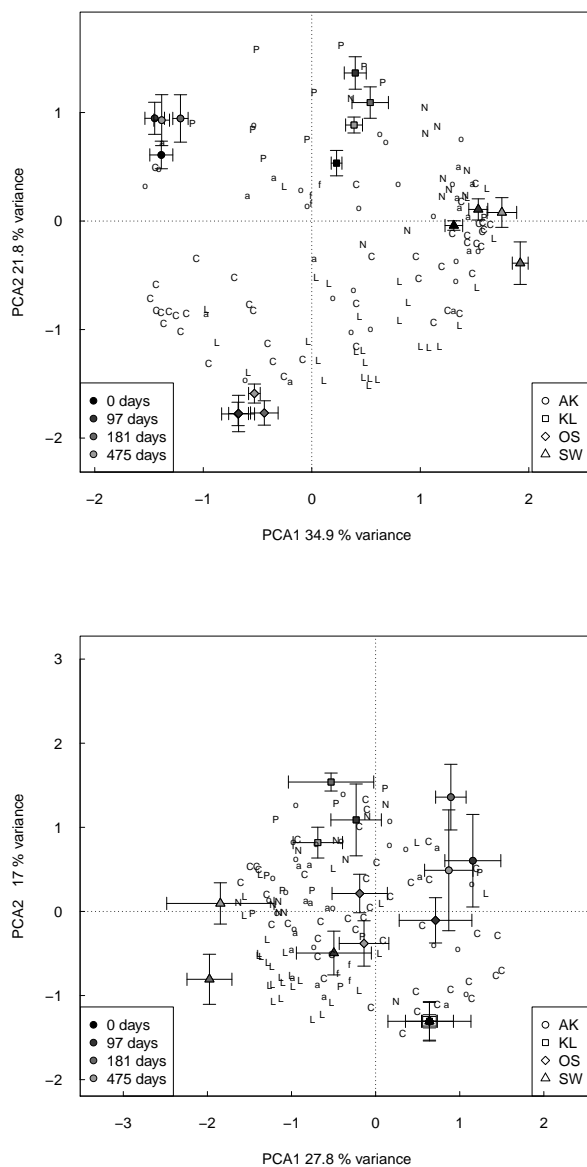


Figure 1: PCA based on 128 peaks quantified in 74 samples. Error bars indicate standard errors (n=4-5). Letters indicate pyrolysis products: C - carbohydrates, L - lignin, P - other phenolic compounds, N - N containing compounds, a - long chained aliphatic compounds (fatty acids, n- alkanes, n-alkenes, phytol

Table 1: Lignin derived and other phenolic pyrolysis products

	Name	RT	MW	integrated fragments	Origin	Class
1	Guaiacol	18.87	124	109+124	L	g
2	Methylguaiacol	20.32	138	123+138	L	g
3	Ethylguaiacol	21.40	152	137+152	L	g
4	Propenylguaiacol	23.29	164	149+164	L	g
5	Vinylguaiacol	23.69	150	135+150	L	g
6	Propenylguaiacol	24.48	164	149+164	L	g
7	Syringol	24.58	154	139+154	L	sy
8	Propenylguaiacol	25.66	164	149+164	L	g
9	Methylsyringol	25.67	168	153+168	L	sy
10	Ethylsyringol	26.39	182	167+182	L	sy
11	Propenylsyringol	27.97	194	179+194	L	sy
12	Vinylsyringol	28.37	180	165+180	L	sy
13	Guaiacolaldehyde	28.40	152	109+152	L	g
14	Propylguaiacol	28.72	166	137+166	L	g
15	Oxo-hydroxy-ethylguaiacol	28.77	182	182	L	g
16	Propenylsyringol	28.91	194	179+194	L	sy
17	Oxo-ethylguaiacol	29.20	166	151+166	L	g
18	Oxo-propylguaiacol	29.36	180	137+180	L	g
19	Propenylsyringol	30.16	194	194+179	L	sy
20	Syringolaldehyde	32.68	182	139+182	L	sy
21	Oxo-hydroxy-ethylsyringol	32.80	212	212	L	sy
22	Guaiacolacetic acid	32.88	182	137+182	L	g
23	Propylsyringol	33.15	196	181+196	L	sy
24	Oxo-propylsyringol	33.32	210	167+210	L	sy
25	Oxopropenylguaiacol	35.30	178	135+178	L	g
26	Hydroxypropenylguaiacol	37.10	137+180	180	L	g
27	Syringolacetic acid	38.78	212	212	L	sy
28	Oxo-propenylsyringol	43.06	208	165+208	L	sy
29	Phenol	21.02	94	65+66+94	Ph	ph
30	4-Methylphenol	22.11	108	107+108	Ph	ph
31	3-Methylphenol	22.22	108	107+108	Ph	ph
32	Ethylphenol	23.38	122	107+122	Ph	ph
33	Propenylphenol	26.93	134	133+134	Ph	ph
34	Propenylphenol	27.76	134	133+134	Ph	ph
35	Propylphenol	31.11	136	151+166	Ph	ph
36	Butylphenol?	31.86	150	107+150	Ph	ph
37	4-Hydroxybenzaldehyde	32.70	122	121+122	Ph	ph
38	Hydroquinone	33.40	110	81+110	Ph	ph

Table 2: Carbohydrate derived pyrolysis products

	Name	RT	MW	integrated fragments	Origin	Class
1	Acetaldehyde	2.06	44	29+44	C	cp
2	Furan	2.35	68	39+68	C	f
3	Methylfuran	2.74	82	81+82	C	f
4	Methylfuran	2.91	82	81+82	C	f
5	Dimethylfuran	3.43	96	95+96	C	f
6	Dimethylfuran	3.66	96	95+96	C	f
7	Vinylfuran	5.01	94	65+94	C	f
8	Unknown furan	6.36	108	107+108	C	f
9	Cyclopentanone	6.99	105?	84+105?	C	cp
10	Methylfuran	7.62	82	53+82+83	C	f
11	2-Oxopropanoic acid, methylester	7.92	102	43+102	C	s
12	1-Hydroxypropanone	9.24	74	43	C	s
13	2-Cyclopenten-1-one	10.26	82	53+54+52	C	cp
14	2-Methyl-2-cyclopenten-1-one	10.51	96	53+96	C	cp
15	1-Hydroxy-2-propanone	10.69	88	57+88	C	cp
16	Unknown	11.38	unk	65+66+94	C	cp
17	3-Furaldehyd	11.57	96	95+96	C	f
18	2(5H)Furanon	11.69	98	55+98	C	f
19	Propanoic acid, methylester	12.10	102	43+102	C	s
20	2-Furaldehyd	12.22	96	95+96	C	f
21	Acetylfuran	12.99	110	95+110	C	cp
22	3-Methyl-cyclopentanone	13.31		67+96	C	cp
23	Dimethylcyclopentenone	13.69	110	67+95+110	C	cp
24	5-Methyl-2-furancarboxaldehyde	14.23	110	109+110	C	f
25	2-Cyclopenten-1,4-dione	14.44	96	54+68+96	C	cp
26	Butyrolactone	15.22	86	56+86	C	cp
27	Unknown	15.56	?	?	C	cp
28	Furanmethanol	15.61	98	98	C	cp
29	5-Methyl-2(5H)-furanone	16.06	98	55+98	C	f
30	Unknown	16.17	unk	110	C	cp
31	1,2-Cyplopentandione	17.51	98	55+98	C	cp
32	Unknown	17.67	unk	42+70	C	cp
33	2-Hydroxy-3-methyl-2-cyclopenten-1-one	18.14	98	98	C	cp
34	3-Methy-1,2-cyclopentanedione	18.42	112	69+112	C	cp
35	Unknown	19.06	unk	58+86+114	C	unk
36	Unknown	19.35	unk	98+126	C	unk
37	Unknown	21.77	unk	116	C	unk
38	Unknown	22.33	unk	44	C	unk
39	Unknown	26.18	unk	57+69	C	unk
40	5-Hydroxymethylfuran1-carboxaldehyde	27.51	126	97+126	C	f
41	Unknown	31.67	unk	73+135	C	unk
42	Laevoglucosan	40.44	172	60+73	C	f

Table 3: Other pyrolysis products quantified

	Name	RT	MW	integrated framents	Origin	Class
1	25:0				Cut	cut0
2	25:1				Cut	cut1
3	27:0				Cut	cut0
4	27:1				Cut	cut1
5	29:0				Cut	cut0
6	29:1				Cut	cut1
7	Myristic acid (14:0)	2.35	68	39+68	lip	fa
8	Palmitic acid (16:0)	2.74	82	81+82	lip	fa
9	Stearic acid (18:0)	2.91	82	81+82	lip	fa
10	N-methyl-pyrrol	6.15	81	80+81	N	N-me-pyr
11	Pyridine	6.90	95	52+79+95	N	p
12	Methylpyridine	7.50	93	66+92+93	N	p
13	Methylpyridine	7.54	93	66+92+93	N	p
14	methylpyridine	9.02	93	66+93	N	p
15	Pyrrol	13.11	67	39+41+67	N	p
16	Methylpyrrol	13.81	81	80+81	N	p
17	Methylpyrrol	14.10	81	80+81	N	p
18	3-Hydroxypyridine	26.52	95	67+95	N	pyridol
19	Indole	26.85	117	89+117	N	ind
20	Methylindole	27.42	131	130+131	N	ind
21	Aceton	2.46	58	43	non	short
22	2-Propenal	2.60	56	55+56	non	short
23	Methanol	2.88	32	29+31+32	non	short
24	3-Buten-2-one	3.39	70	55+70	non	short
25	2,3-Butandione	3.67	86	69+86	non	short
26	3-Penten-2-one	3.89	86	69+86	non	short
27	Toluene	4.54	92	91+92	non	ar
28	2-Butanal	4.56	70	69+70	non	short
29	2,3-Pentadione	4.77	100	57+100	non	short
30	Hexanal	5.16	82	56+72+82	non	short
31	Xylene	5.94	106	91+105+106	non	ar
32	Xylene	6.09	106	91+105+106	non	ar
33	Xylene	6.20	106	91+105+106	non	ar
34	Xylene	6.99	105?	84+105?	non	ar
35	Limonene	7.22	?	93	non	ter
36	1-Penten-3-one	11.28	84	55+84	non	short
37	Methoxytoluene	11.78	122	121+122	non	ar
38	Indene	12.64	116	115+116	non	ar
39	Benzaldehyde	13.35	106	77+106	non	ar
40	1-Methyl-4-methoxybenzene	15.98	?	?	non	ar
41	Phytol	20.00	?	95+123	phytol	phytol
42	Unknown	20.85	unk	?	unk	unk
43	Unknown	20.86	unk	?	unk	unk
44	Unknown	22.43	unk	98+128	unk	unk
45	Unknown aliphatic	22.82	unk	58+71	unk	al
46	Hexan2,4dion	23.92	114	56+84+114	unk	o
47	Dihydrobenzofuran	26.19	120	91+119+120	unk	bf
48	Unknown	27.76	unk	138	unk	unk

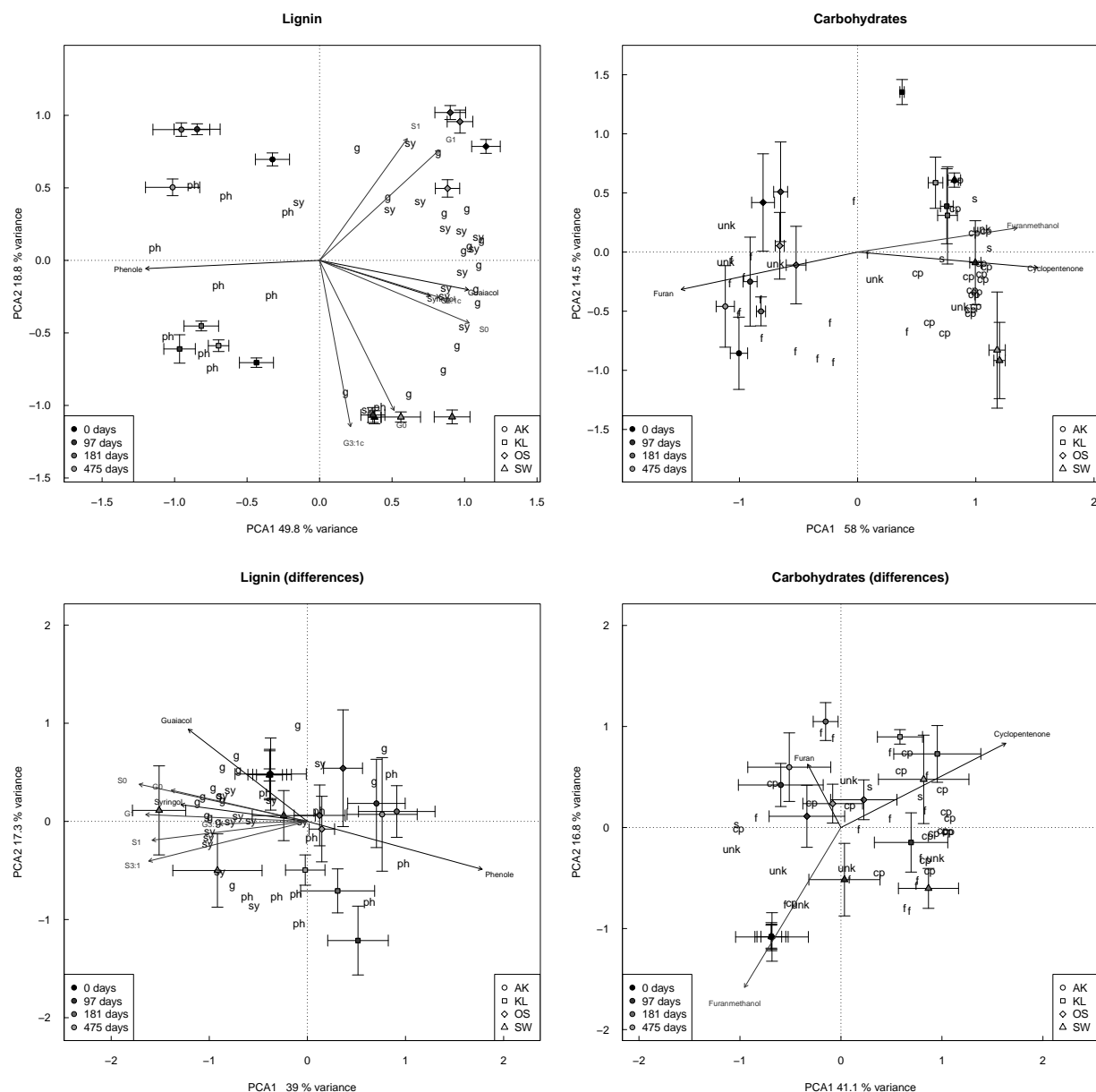


Figure 2: The upper left graphs shows a PCA of relative contributions of lignin and phenol pyrolysis products to the sum of these products, the lower left graph shows the difference of this relative contribution to initial contributions. The both graphs on the right hand show the same relations for carbohydrate derived pyrolysis products. Sample means (n=4-5) and standard errors are stated as indicated in the plot legend. Letters indicate pyrolysis products (g - guaiacol lignin, sy - syringol lignin, ph - phenolic compounds, cp - cyclopentenone-type and f - furan type carbohydrate markers). Black arrows indicate fits for %TIC sum of compound classes (guaiacol and syringol lignin, other phenolic compounds, furan- and cyclopentenone-type carbohydrate markers), grey arrows indicate selected individual markers (G1/S0 - guaiacol/syringol, G/S1 - methylguaiacol/-syringol, G3:1/S3:1 - Propenylguaiacol/syringol.) The lower graph shows a PCA based on differences to initial peak abundance.

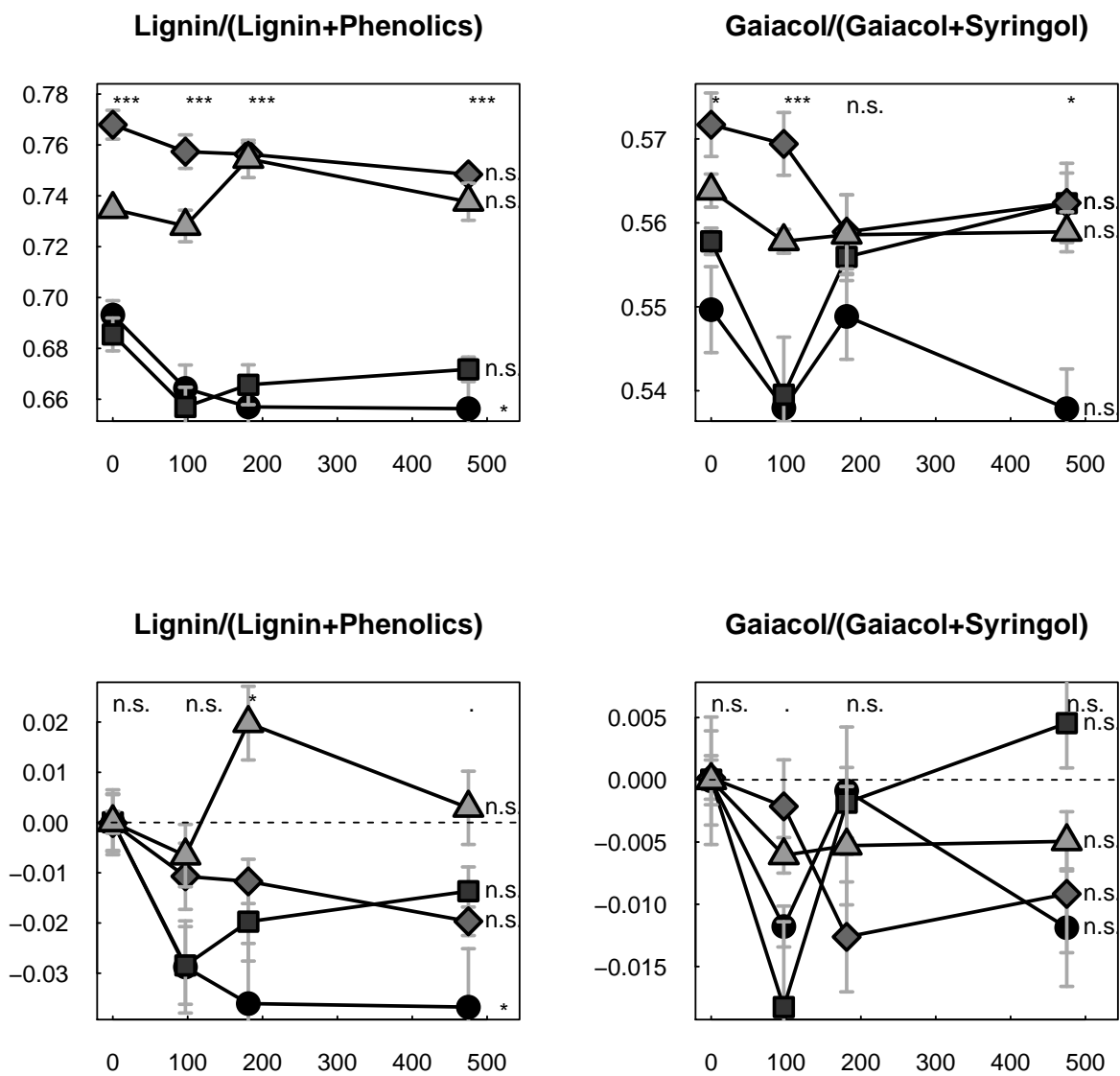


Figure 3:

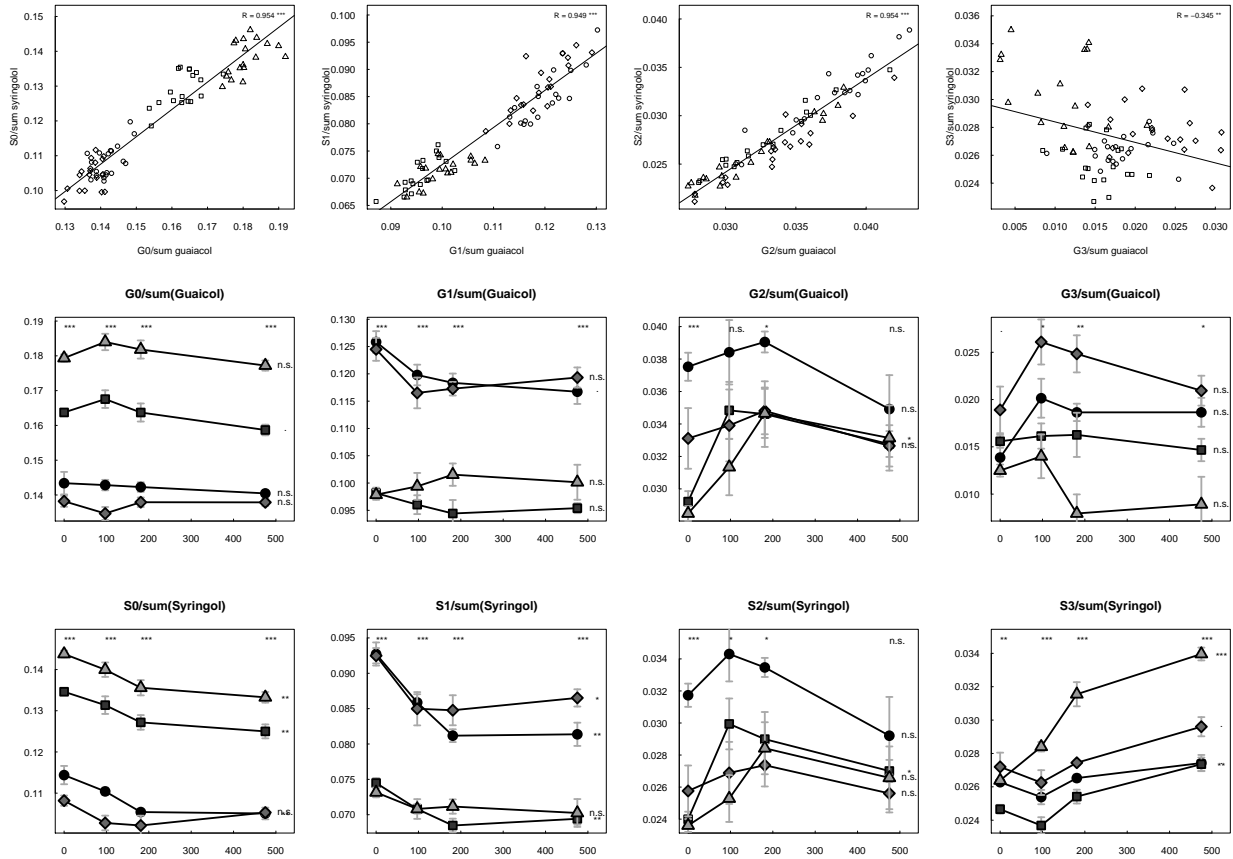


Figure 4: Lignin side chains occur in the same ratios for both guaiacol and syringol lignin, but differences in the content of -H and -CH<sub>3</sub> side chains were found.



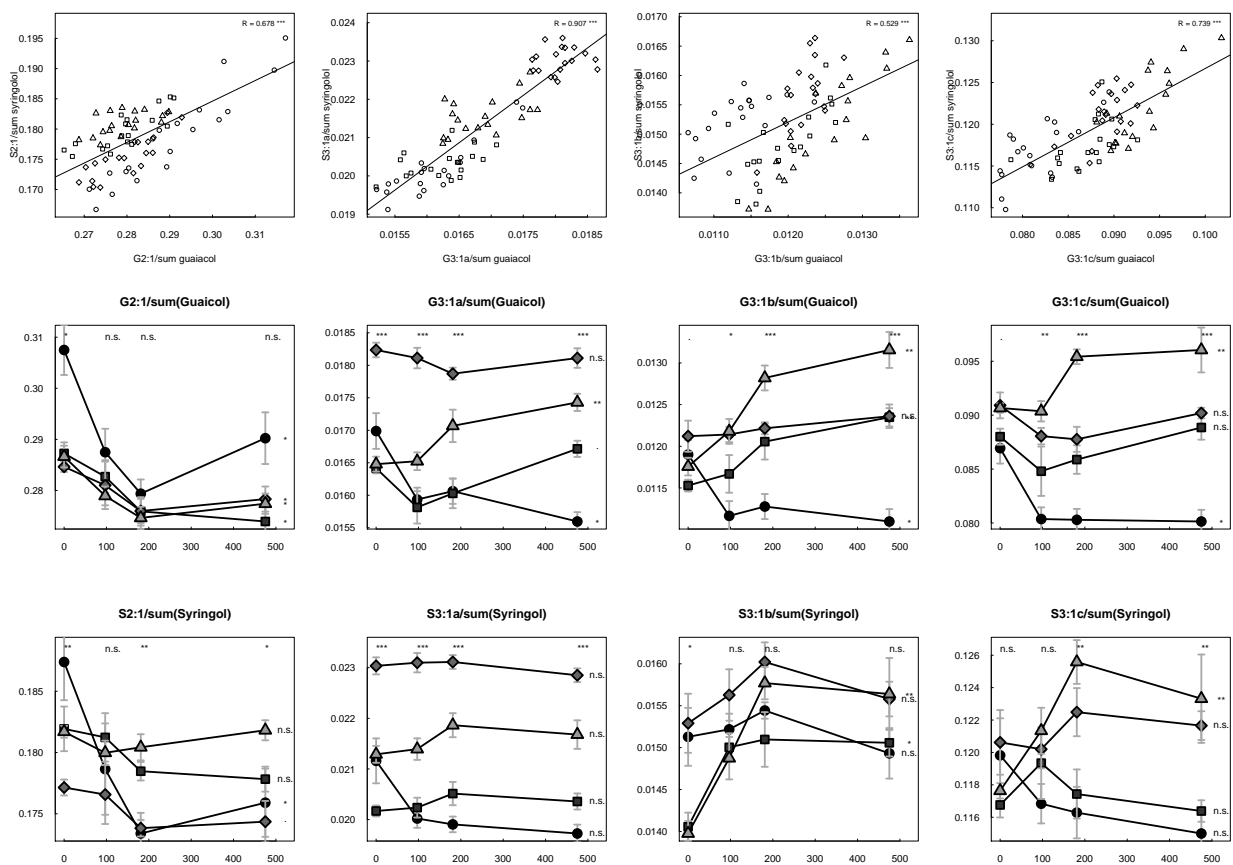


Figure 5: Lignin side chains occur in the same ratios for both guaiacol and syringol lignin, but differences in the content of -H and -CH<sub>3</sub> side chains were found.

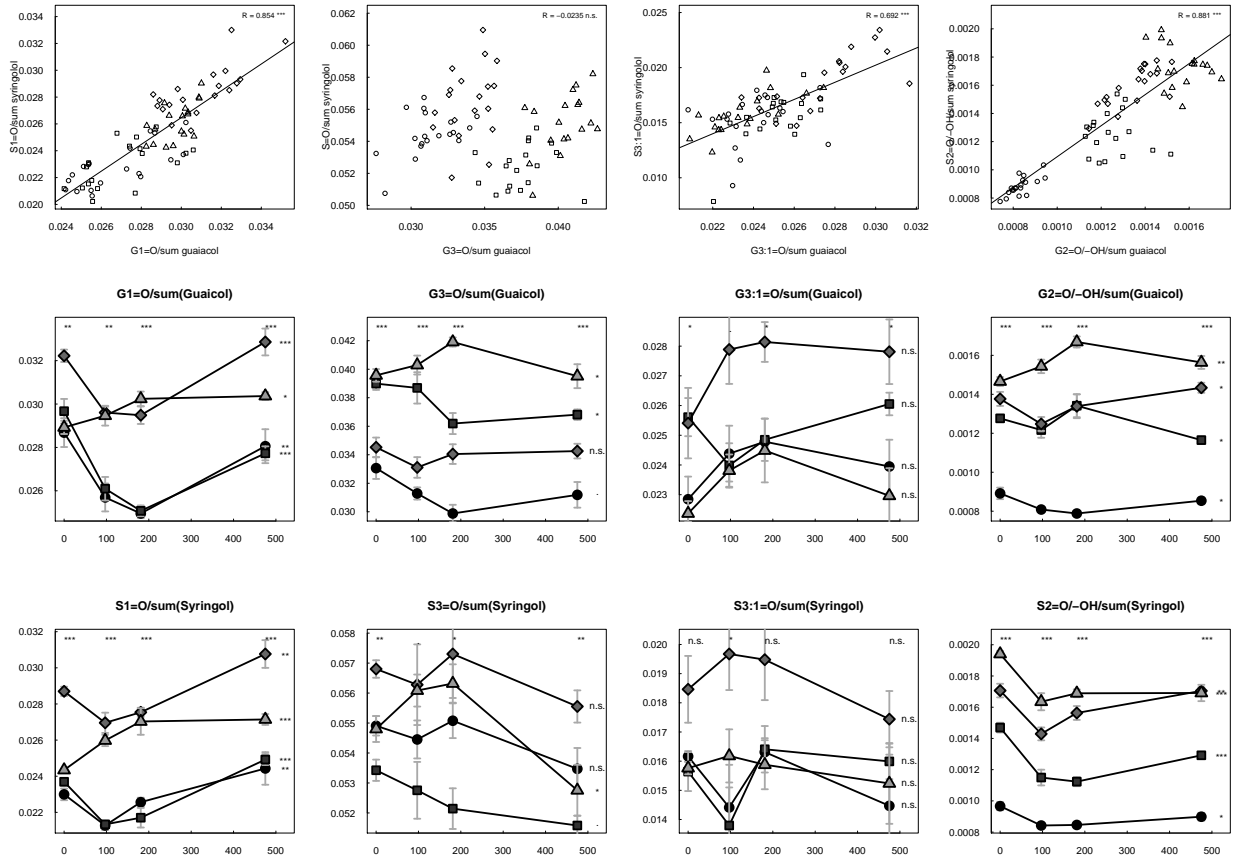


Figure 6: Lignin side chains occur in the same ratios for both guaiacol and syringol lignin, but differences in the content of -H and -CH<sub>3</sub> side chains were found.

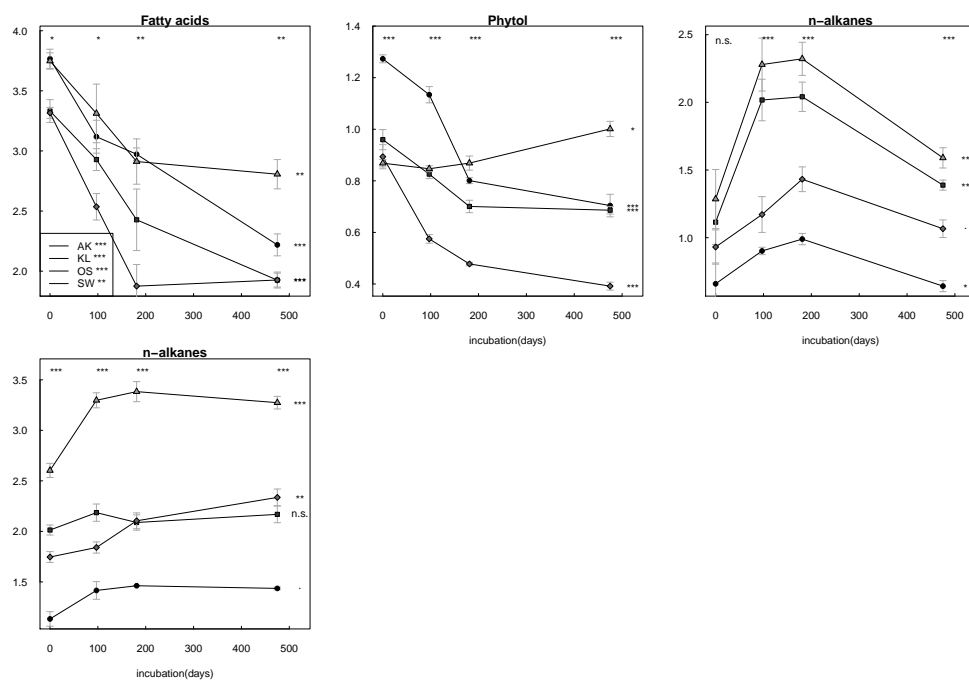


Figure 7: Trends for lipophilic compounds found in isolated lignin. Two samples were excluded due to contaminations.

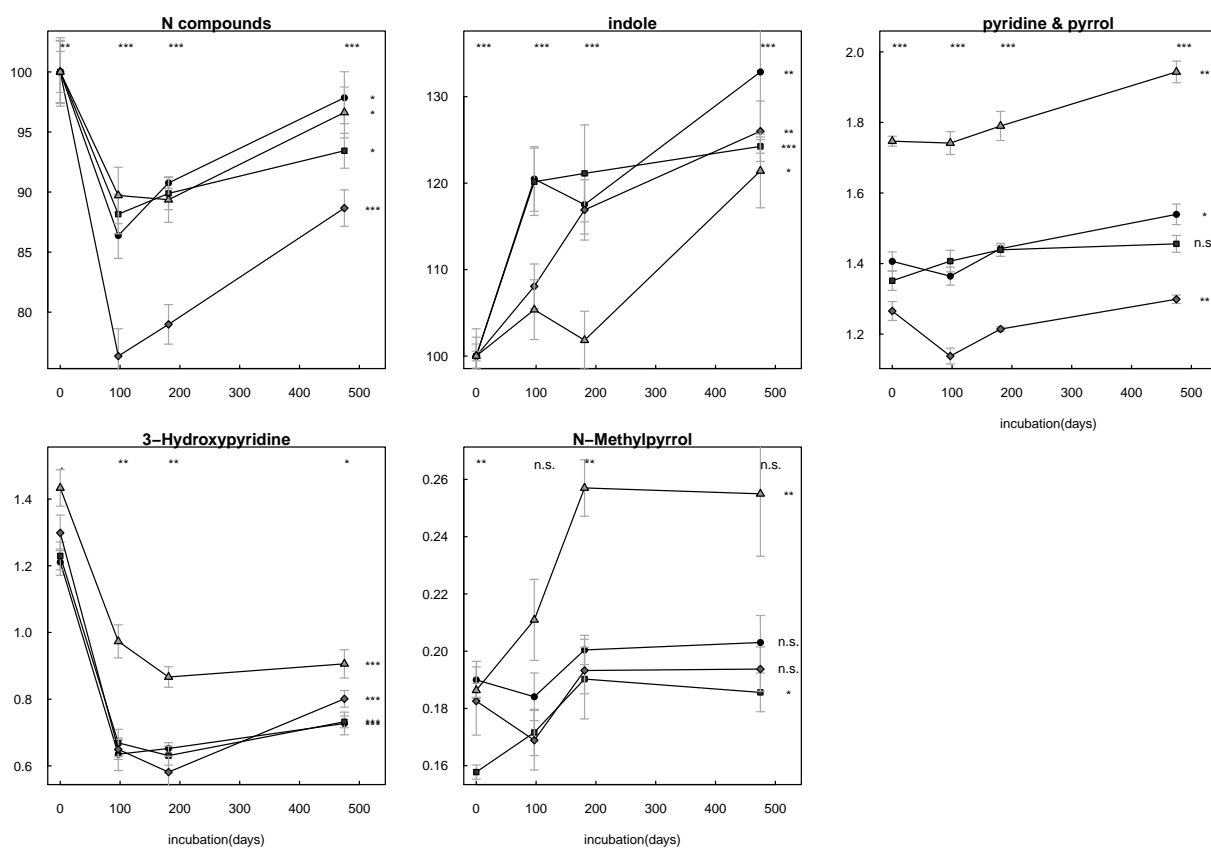


Figure 8: Trends for nitrogen compounds found in isolated lignin. Two samples were excluded due to contaminations.